Three-Dimensional Models for β-Adrenergic Receptor Complexes with Agonists and Antagonists

Kristina E. Furse and Terry P. Lybrand*

Department of Chemistry & Center for Structural Biology, 5142 Biosciences/MRB III, Vanderbilt University, Nashville, Tennessee 37232-8725

Received March 28, 2003

Molecular modeling methods have been used to construct three-dimensional models for agonist and antagonist complexes with β-adrenergic receptors. The recent rhodopsin crystal structure was used as a template in standard homology modeling methods. The rhodopsin-based homology models were assessed for agreement with experimental results for β-adrenergic receptors, and compared with receptor models developed using de novo modeling techniques. While the de novo and homology-derived receptor models are generally quite similar, there are some localized structural differences that impact the putative ligand-binding site significantly. The de novo receptor models appear to provide much better agreement with experimental data, particularly for receptor complexes with agonist ligands. The de novo receptor models also yield some interesting and testable hypotheses for the structural basis of β-adrenergic receptor subtype ligand selectivity.

Introduction

G-protein-coupled receptors (GPCRs) comprise a superfamily of proteins that play a key role in signal transduction in many cells and are implicated in control or regulation of a wide array of biological functions. Thus, these receptors are important therapeutic targets in a variety of disease states. Most members of this superfamily are thought to share a common topology, a seven-transmembrane helix bundle, even though sequence conservation across the superfamily is minimal. Like many integral membrane proteins, GPCRs are challenging molecules to study experimentally. It is particularly difficult to obtain large amounts of most GPCRs, which makes high-resolution structural characterization nearly impossible. Due to these difficulties, great importance has been placed on indirect structural evidence obtained from a variety of biophysical techniques, as well as detailed sequence analysis and molecular modeling studies.

These data and computational techniques have been used to create and refine an almost limitless number of published and unpublished theoretical three-dimensional (3D) models over the past decade (for recent reviews, see refs 1 and 2). Many early models were generated using homology modeling techniques with bacteriorhodopsin as a structural template.[3,4] When the validity of a bacteriorhodopsin structural template was questioned,[5,6] many models were instead based on automated or de novo design techniques. While these models have been extremely useful in the generation of hypotheses and the design and interpretation of new experiments, they are still quite speculative and must be used with some caution. The recent publication of the first high-resolution crystal structure for rhodopsin,[7] a GPCR superfamily member, provides the option of homology modeling to generate 3D models based more solidly on detailed structural information.

* To whom correspondence should be addressed. Phone: (615) 343-1247. Fax: (615) 936-2211. E-mail: terry.p.lybrand@vanderbilt.edu.

While the rhodopsin structure represents a major breakthrough in our understanding of these important proteins, numerous recent publications caution against the indiscriminant use of this crystal structure as a general GPCR template.[8−10] In previous work, we have shown that the rhodopsin structure is not an appropriate template for GPCRs that bind peptide ligands in the extracellular loop domain, such as the cholecystokinin A receptor.[11] Even when the scope is narrowed to rhodopsin-like Class A GPCRs which bind small molecule ligands, there are several issues surrounding the use of rhodopsin as a template that must be considered. First and foremost, the crystal structure is a snapshot of rhodopsin in its inactive, nonsignaling state.[7,12] The "ligand" in this ground-state structure, 11-*cis*-retinal, functions as an inverse agonist to diminish activity levels below that of retinal-free opsin, which is crucial for rhodopsin's competent function as a single-photon detector.[12] The details of the conformational changes that rhodopsin or other GPCRs undergo upon activation are still somewhat unclear, but biophysical studies suggest that nontrivial conformational changes do occur.[13−17] Under physiological conditions, these receptors are thought to be in a constant state of conformational flux, resulting in a complex equilibrium of multiple, rapidly interconverting conformations that represent a range of activity levels.[18] As a result, it is questionable if the rhodopsin crystal structure is completely appropriate to use in modeling GPCR−agonist complexes in particular.

Additionally, a number of structural features of rhodopsin were somewhat surprising, such as the highly ordered extracellular region, including a structured globular amino terminus and β-sheet moieties in the loops, and striking bends, bulges, kinks, and stretches of 3_{10} helix in the transmembrane domains.[7] Since there is little sequence similarity between rhodopsin and most other GPCRs in the extracellular domains, and only limited sequence similarity in most transmembrane

10.1021/jm0301437 CCC: $25.00
Published on Web 09/17/2003

regions (e.g., ~22% sequence identity between rhodopsin and β_2-receptor in the transmembrane domains), it is not clear which of these structural features may be unique to rhodopsin and the opsins, and which may be more general. To address these concerns, several different strategies may be used. One approach, applied recently in several GPCR modeling studies, uses the rhodopsin crystal structure in conventional homology modeling exercises to generate 3D models for GPCRs in their ground state, with subsequent structural refinements to model the conformational changes that accompany receptor activation.[8,10] While this is an inherently attractive strategy, it is problematic at present because there is not yet enough experimental data regarding the detailed conformational changes that lead to receptor activation to guide the modeling process. Therefore, we have chosen to use available experimental data for GPCR−agonist interactions as spatial constraints in refinement of plausible agonist complexes. We compare details of models developed using this constraint-based, "de novo" modeling approach with corresponding models derived directly from the rhodopsin crystal structure, to determine if constraint-based models may be better able to provide useful information regarding receptor−agonist complexes in particular.

We report here a set of updated models for β-adrenergic receptors (β_1, β_2, β_3), refined on the basis of recent experimental data as well as structural cues from the rhodopsin crystal structure, and utilize them to investigate questions of stereoselective ligand binding and receptor subtype ligand selectivity. The de novo models were generated originally from packing calculations for a set of idealized α-helices corresponding to the seven transmembrane helical segments.[6] Helix positioning and tilt angles were further adjusted using a compilation of 2D electron micrographs of frog rhodopsin,[19] with subsequent extensive structural refinement using data from a variety of biophysical and ligand-binding experiments for β-adrenergic receptors as structural constraints.[6] These earlier models served as the starting point for the new de novo models reported here. Corresponding homology models for each receptor−ligand complex were derived directly from the rhodopsin crystal structure, and refined to remove stereochemical violations and bad steric contacts, but with no additional constraints applied.

After rhodopsin, the β-adrenergic receptors are among the most thoroughly studied and well characterized GPCRs, so they serve as an excellent test case system. Several key binding site contacts have been established for a variety of agonists using various experimental techniques.[20,21] The binding site orientation of several antagonists has also been characterized in affinity labeling studies.[22,23] However, a number of important issues for β-adrenergic receptors are still unresolved. For example, the structural basis for the strong stereoselective ligand-binding preference for β-adrenergic receptors has not been well established for antagonists. The detailed basis for β-adrenergic receptor subtype ligand-binding selectivity is also poorly understood at present. Detailed understanding of the basis for receptor subtype ligand-binding selectivity could be exploited to help design drugs that are exquisitely selective for one target receptor, potentially eliminating side effects that arise from unintended interactions of the drug molecule with receptors that are closely related to the target. For example, β_3-adrenergic receptors are of great interest as prospective targets for anti-obesity and anti-diabetic therapeutics.[24] An ideal therapeutic agent would target the β_3-receptor without stimulating β_1- or β_2-receptors, thereby avoiding cardiovascular and respiratory side effects. The question of receptor subtype selectivity is necessarily a subtle one, as it involves exploitation of small differences in very similar receptors. Receptor subtypes often exhibit sequence identity greater than 70%, suggesting significant structural similarity. Thus, we have used our best β-receptor models to attempt to provide additional insight into the structural basis of stereoselective ligand binding and receptor subtype ligand-binding selectivity.

Results and Discussion

General Model Characteristics. Standard homology models were generated using both automated and manual model building techniques. The rhodopsin backbone coordinates were kept fixed initially, with amino acid side-chain replacement to generate the β-receptor sequences. Side-chain rotamers were selected using a systematic search of allowable conformations tabulated in a standard rotamer database. The resulting homology models were refined with limited energy minimization and low-temperature molecular dynamics to relieve unfavorable steric interactions. The resultant homology models closely match the rhodopsin backbone conformation, with an RMS deviation for backbone atoms of 0.6 Å, and have acceptable stereochemical parameters and side-chain packing densities.

The de novo model construction strategy has been reported previously.[6,25] Originally, these models were constructed starting with seven idealized α-helices corresponding to each transmembrane segment. Manual and semi-automated model building procedures were used to explore all possible topological arrangements for packing seven helices into a compact bundle. Only those seven-helix bundle arrangements that clustered experimentally documented binding site residues in a localized region of the bundle interior (i.e., a putative ligand-binding site) were selected for further refinement. This strategy yielded a small number of receptor models that exhibited energetically reasonable backbone conformations, stereochemistry, and side-chain packing interactions, while also forming plausible ligand-binding sites consistent with available experimental data.

In the present work, adjustments were made to those earlier de novo models, based on additional data from recent experiments and some features observed in the rhodopsin crystal structure. Specifically, the amino-terminal (i.e., extracellular) end of the third transmembrane helix (TM3) was extended by one full turn, as suggested by the rhodopsin structure. This modification places residue C106, which forms a highly conserved disulfide bond in the extracellular domain of most GPCRs, at the beginning of TM3.

Highly conserved proline residues in GPCRs likely induce notable kinks in the transmembrane helices and may serve important functional roles in signal transduction.[26] Several proline kinks are observed in the rhodopsin structure. Unfortunately, the proline residues

are not completely conserved between rhodopsin and the β_2-receptor, and proline kinks in the sixth and seventh transmembrane helices in rhodopsin are more dramatic than those observed in other protein structures. It is unclear whether these dramatic proline kinks reflect intrinsic sequence-dependent attributes of rhodopsin, or rather the inactive (i.e., inverse agonist-bound) conformation of the rhodopsin structure. Therefore, proline kinks in TM2 (P88), TM6 (P288), and TM7 (P323) were adjusted manually by modifying the ϕ and ψ backbone angles of residues at positions $i - 1$ and $i - 2$ relative to proline, so as to adopt values observed in a detailed analysis of proline kinks in a collection of high-resolution protein crystal structures.[27]

The rhodopsin structure has a short α-helical segment extending from the cytosolic end of TM7 that lies parallel to the lipid bilayer surface. Sequence alignment results suggest that β-receptors may also possess this helical segment, so it was generated manually using the corresponding region of the rhodopsin structure as a template. The resulting helix segment places the highly conserved residue F332 in the interior of the transmembrane helix bundle domain, while R333 is positioned favorably for interaction with the cytosolic membrane phospholipid headgroups.

All of these local helical adjustments introduced some bad steric contacts and reoriented some important ligand-binding residues slightly away from the putative ligand-binding pocket. Recent data suggest that residues Y199 and S203 are accessible to the binding site as well,[22,28] so the transmembrane helices were rotated slightly to reposition residues D113, Y199, S203, S204, S207, and F290 into the binding pocket. The fifth transmembrane helix was also shifted slightly (∼1 Å) toward the cytosolic surface to better reflect the TM5 register observed in the rhodopsin structure. The extracellular and cytosolic loops were generated using an automated loop generation procedure.[11] Peptide segments corresponding to the amino- and carboxy-terminal halves of each loop were constructed in extended conformation and attached to the ends of the appropriate transmembrane helices. Weak harmonic constraints were then applied during the course of short, low-temperature molecular dynamics simulations to close the loop segments, forming a trans amide bond at the ligation site. This model has improved side-chain interactions and packing compared to the earlier de novo models, even though the overall backbone RMSD relative to the previous de novo receptor models is modest (∼1.8 Å).

After initial model construction, epinephrine was docked manually to create an agonist complex, using documented receptor interactions (e.g., D113 with the ligand's protonated amine, S204 and S207 with the catechol hydroxyls, etc.) to guide placement of the ligand in the binding pocket. The complex was then refined with limited energy minimization and short, low-temperature molecular dynamics simulations to relieve any residual bad steric contacts. Harmonic restraints were applied to all backbone atoms in the transmembrane domain to minimize potential distortion of helices during in vacuo structural refinement.

The resultant de novo model and the bovine rhodopsin crystal structure are fundamentally quite similar in the transmembrane domain (Figure 1), exhibiting a backbone RMS deviation of 2.8 Å. The extracellular domains, on the other hand, are noticeably different. GPCRs are thought to exhibit a conserved disulfide link between the top of TM3 and the second extracellular loop (ECL2). This was indeed shown to be the case with the rhodopsin crystal structure. Unlike most GPCRs, β-adrenergic receptors contain three cysteine residues in ECL2 which participate in two disulfide bonds—one analogous to the prototypical GPCR link between TM3 and ECL2 (C106 in TM3 and C191 in ECL2), plus a second disulfide bond that lends additional structure to the loop conformation (C184 and C190 within ECL2).[29,30] This pairing of extracellular cysteines results in a short, five-residue chain between the top of TM5 and the disulfide cross link to TM3 (Figure 1A), as opposed to a 12-residue segment that would exist at this position if the conventional rhodopsin disulfide cross-link pattern was present. The conformational restriction imposed by this short tether positions several loop residues in close contact with the ligand-binding site, giving additional structure to the top of the binding pocket. This "roof" does not seem to affect small agonists, as they bind lower in the pocket, but does appear to play a role in the binding of antagonists as well as agonists containing larger N-substituents. Though the stretch of residues between the conserved disulfide bond and the top of TM5 is quite a bit longer in rhodopsin, the crystal structure showed the second extracellular loop to have β-strand character and to penetrate fairly deeply into the binding site, making direct contact with retinal (Figure 1B). The corresponding loop region in the de novo model cannot penetrate as deeply into the helix bundle interior, as the two disulfide bonds restrict conformational flexibility and tether the loop more tightly to the top of TM5. Direct adoption of the loop conformation and position from the rhodopsin structure precludes formation of the distinct cysteine pairings observed for β-adrenergic receptors[30] and prohibits binding of all but the smallest agonists to the β_2-receptor homology model, since this region of the second extracellular loop in fact occupies the upper region of the ligand-binding pocket, with considerable penetration of loop residues into the ligand-binding pocket (Figure 2).

Ligand Binding. The endogenous ligand epinephrine (Figure 3A), the prototypical agonist isoproterenol (Figure 3B), and the β_2-selective agonist TA-2005 (Figure 3C) were docked in the β_2-receptor model to investigate typical agonist interactions. Propranolol (Figure 3E), aminoflisopolol (AmF) (Figure 3F), and the carazolol derivative *p*-(bromoacetamidyl)benzylcarazolol (*p*BABC) (Figure 3G) were chosen as typical neutral antagonists for docking exercises with the receptor models. Docked complexes were also generated for the inverse agonist ICI-118,551 (Figure 3H), since it should be possible, in principle, to accommodate inverse agonists in a strict rhodopsin homology model with no difficulty. Both erythro isomers of ICI-118,551 (2*R*,3*S*-ICI-118,551 and 2*S*,3*R*-ICI-118,551) were studied, since it is not known definitively which isomer binds more tightly. Extensive conformational analysis was performed for the ligands to ensure that final results were not unduly biased by selection of only one or two low-energy ligand conformers, and manual rigid ligand-

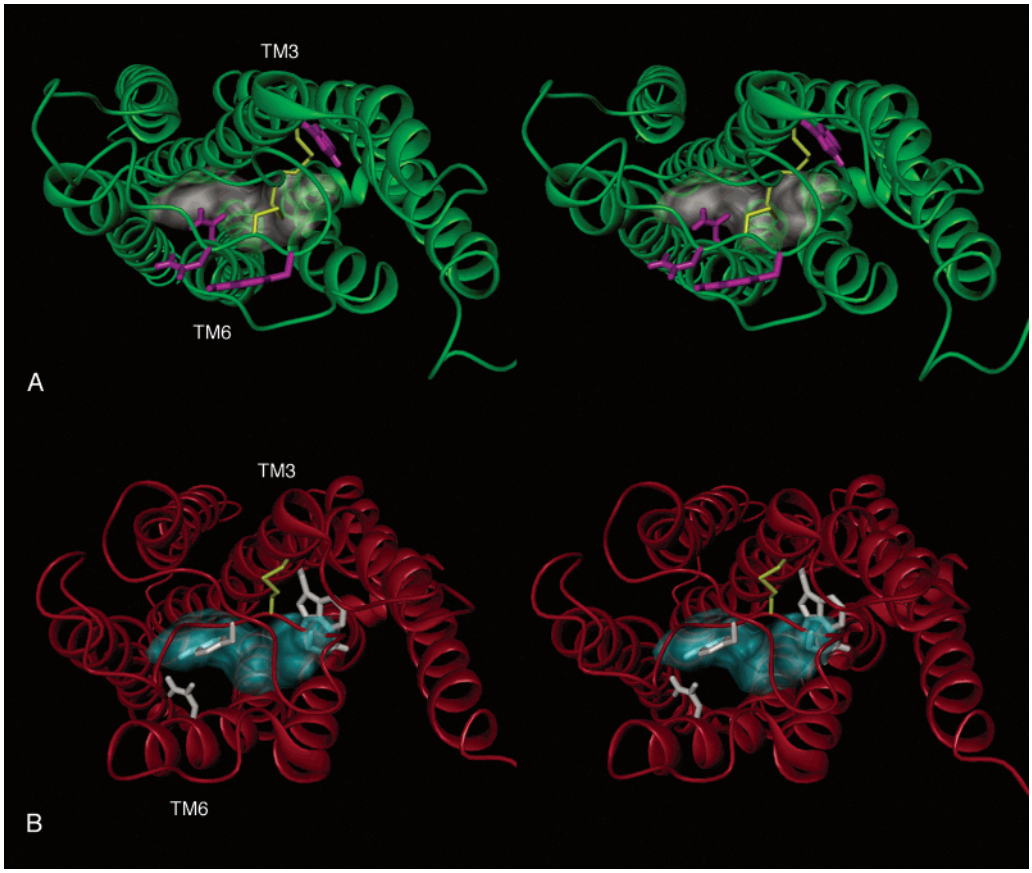

Figure 1. Top (extracellular) stereoviews of identical orientations of (A) the de novo β_2-adrenergic receptor model, and (B) the homology model. (A) A translucent, reduced surface of the β_2-AR-selective agonist TA-2005 is displayed in white, indicating the region of the putative ligand-binding site. Receptor backbones are represented in green with residues W109 in TM3 and N293 in TM6, as well as second extracellular loop residues N183 and Y185, displayed in magenta. The second extracellular loop contains two disulfide bonds (yellow) characteristic of β-adrenergic receptors. (B) The surface and residues are the same as shown in panel A, with the backbone in red, residues highlighted in white, and ligand surface in cyan. The homology model complex includes the second extracellular loop conformation observed in the rhodopsin crystal structure, with its single disulfide bond highlighted in yellow. Panel B illustrates the steric clashes characteristic of homology model complexes with larger agonists and antagonists. As can be seen clearly in this figure, the rhodopsin loop conformation precludes formation of the second disulfide bond. The molecular surface was generated with the MSMS[59] program. Figures 1, 2, and 4−9 were generated with the Dino program.[60]

docking exercises were performed for all low-energy conformers for each molecule. Automated docking methods were also employed to search for alternative ligand-docking orientations that might satisfy experimental constraints, and to provide independent, unbiased corroboration of the manual ligand-docking results. Multiple low-temperature molecular dynamics trajectories were then run for each docked complex to identify stable receptor−ligand interactions. Isoproterenol exhibits a 10-fold greater stereoselective binding preference than epinephrine for the β_2-receptor, so each stereoisomer of isoproterenol was treated as a distinct ligand in an attempt to explain this observation. For the other ligands, only the preferred stereoisomer of each molecule was examined.

Initial placement of ligands in manual docking exercises was guided by key receptor−ligand interactions suggested by experimental evidence.[20,21] The protonated amine of all of ligands was placed near D113 in TM3, and all receptor−ligand complexes maintained the charge-reinforced hydrogen bond during dynamics. The catechol, or catechol-equivalent end of the ligand, was oriented toward TM5, in the pocket formed by TM3, TM5, and TM6. With these initial placement criteria, N293 in TM6 emerged as the hydrogen bond partner in the de novo models for the β-hydroxyl of every ligand except *S*-isoproterenol, which is the weaker binding isomer. Beyond these general features, contacts are specific to agonists and neutral antagonists, which exhibited somewhat different binding modes.

Agonists. Agonist complexes with isoproterenol and TA-2005 are shown in Figures 4 and 5. In the de novo model complexes with small catechol agonists, the ligand aromatic ring interacts with residues W286 and F290 from the aromatic wall region of TM6,[20,31] and V114 and T110 on the opposite side of the binding pocket in TM3, while the *N*-alkyl substituents fit in a pocket formed by F289 and H296 in TM6, and N312 in TM7. The catechol hydroxyl groups form hydrogen bonds with two of the TM5 serines, *m*-OH with S204 and *p*-OH with S207. The D113 and serine contacts combine to give a three-point positional constraint that dramatically limits the conformational and orientational freedom of the ligand. When these three interactions are established for isoproterenol, the *R* isomer is ideally positioned to form a hydrogen bond between the hydroxyl group attached to the chiral side-chain carbon (β-OH) and N293. The same three-point constraint for low-energy conformers of the *S* isomer orients the β-OH into TM6 below N293, toward the residues that com-

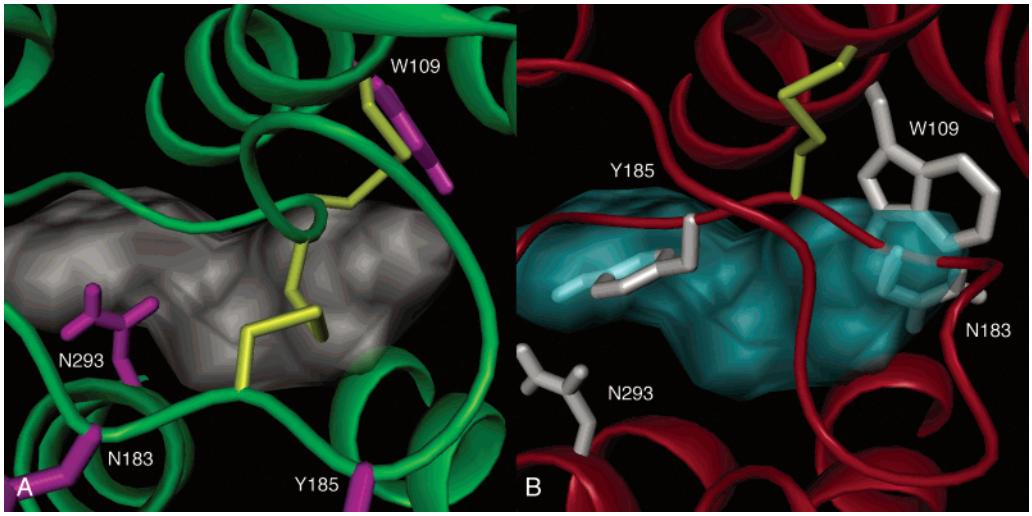

Figure 2. Close-up views of the (A) de novo and (B) homology model complexes shown in Figure 1. The backbone of the second extracellular loop of the homology model is shown penetrating the surface representing the β_2-AR selective agonist TA-2005 (cyan), submerging the α, β, and γ carbons of loop residue N183. Loop residue Y185, and W109 in TM3, exhibit significant steric clashes with the ligand as well. The conformation of the sixth transmembrane helix (TM6) determines the position of N293 in the two models. In the de novo model, this residue forms a hydrogen bond with the side-chain hydroxyl of TA-2005, with a donor−acceptor distance of 3.1 Å. The displacement of N293 in the homology model precludes formation of this hydrogen bond, with a donor−acceptor distance of 6.4 Å.

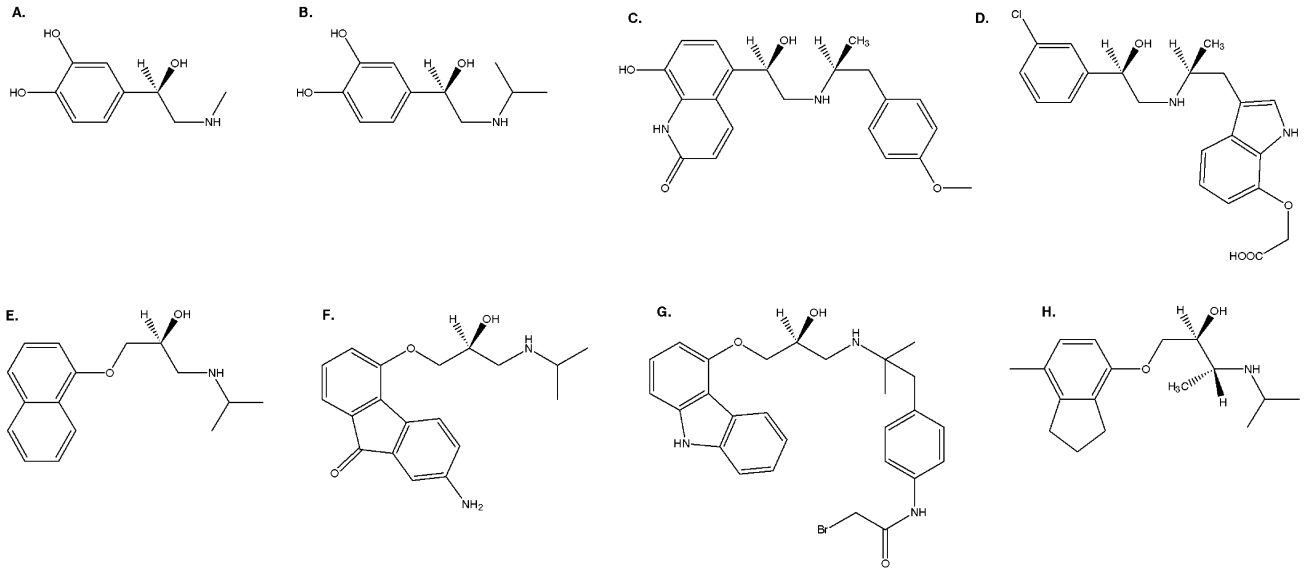

Figure 3. β-adrenergic agonists, antagonists, and inverse agonist used in docking exercises: (A) (*R*)-epinephrine {(1*R*)-1-(3,4-dihydroxyphenyl)-2-(methylamino)ethanol}, (B) (*R*)-isoproterenol {(1*R*)-1-(3,4-dihydroxyphenyl)-2-(isopropylamino)ethanol}, (C) TA-2005 {8-hydroxy-5-[(1*R*)-1-hydroxy-2-[[2-(4-methoxyphenyl)-(1*R*)-1-methylethyl]amino]ethyl]-2-oxoquinoline}, (D) AJ-9677 {[[3-[(2*R*)-2-[[(2*R*)-2-(3-chlorophenyl)-2-hydroxyethyl]amino]propyl]-1*H*-indol-7-yl]oxy]acetic acid}, (E) (*S*)-propranolol {(2*S*)-1-(isopropylamino)-3-(1-naphthyloxy)-2-propanol}, (F) (*S*)-aminoflisopolol {4-[(2*S*)-2-hydroxy-3-isopropylaminopropoxy]-7-amino-fluorenone}, (G) (*S*)-*p*-(bromoacetamido)benzylcarazolol {4-[(2*S*)-2-hydroxy-3-[[2-[4-(bromoacetamido)phenyl]-1,1-dimethylethyl]-amino]propoxy]carbazole}, and (H) ICI-118,551 {*erythro*-(2*S*,3*R*)-1(7-methylindan-4-yloxy)-3-isopropylaminobutan-2-ol}.

prise the aromatic wall, where there are no viable hydrogen bond partners. If the β-OH hydrogen bond with N293 is imposed as an additional constraint in docking the *S* isomer, extremely unfavorable van der Waals interactions are introduced between the *N*-isopropyl substituent and the peptide backbone atoms of T110 and D113 in TM3. An extremely high-energy conformer of *S*-isoproterenol (>20 kcal/mol above the global minimum) must be adopted to relieve the steric clashes while simultaneously maintaining all four specific ligand interactions with the receptor.

Comparable ligand−receptor interactions are observed for agonists in the homology model, except that N293 is shifted 3.5−4.0 Å away from the ligand-binding pocket (Figures 1B and 2B) due to differences in TM6 tilt and twist in the helix bundle, and thus cannot form a stereoselective hydrogen bond with the agonists. Since this stereoselective hydrogen bond with N293 is well established experimentally for agonists like isoproterenol,[32] this represents a serious flaw in the homology model that can be corrected only by significant reorientation of TM6.

The larger, non-catechol agonist, TA-2005 (Figure 3C), was evaluated to assess its β_2 subtype selectivity (discussed below). Its larger chromophore settled lower in the binding site during refinement, making an

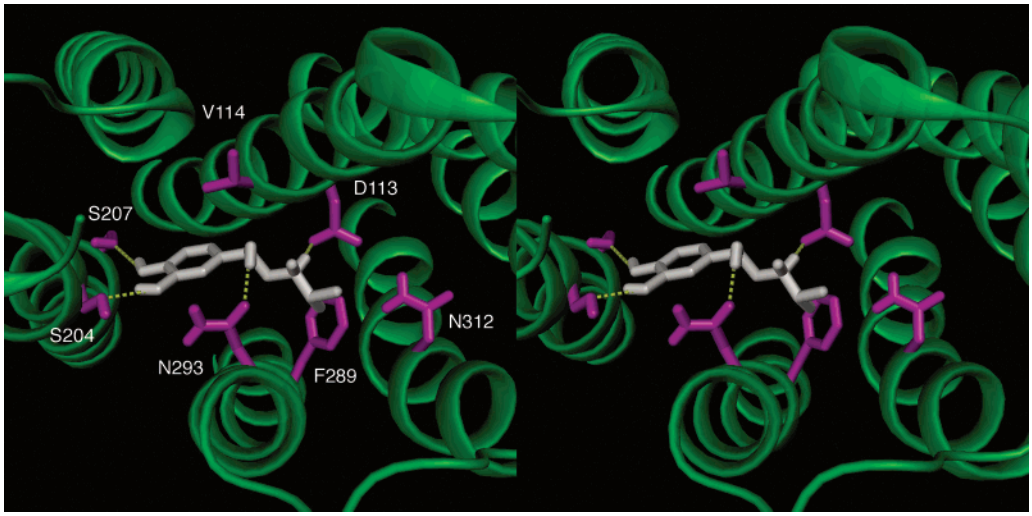

Figure 4. Top (extracellular) stereoview of the (*R*)-isoproterenol complex with de novo β_2-AR model. The ligand is displayed in white, and key binding site residues are shown in magenta. Hydrogen bonds are represented with dashed yellow lines. Key contacts include a charge reinforced hydrogen bond between the protonated amine and D113 in TM3, hydrogen bonds between the catechol hydroxyls, *m*OH and *p*OH, with S204 and S207 in TM5, and a hydrogen bond between ligand side-chain hydroxyl and N293 in TM6. The ligand also makes van der Waals contact with V114 in TM3, F289 in TM6, and N312 in TM7.

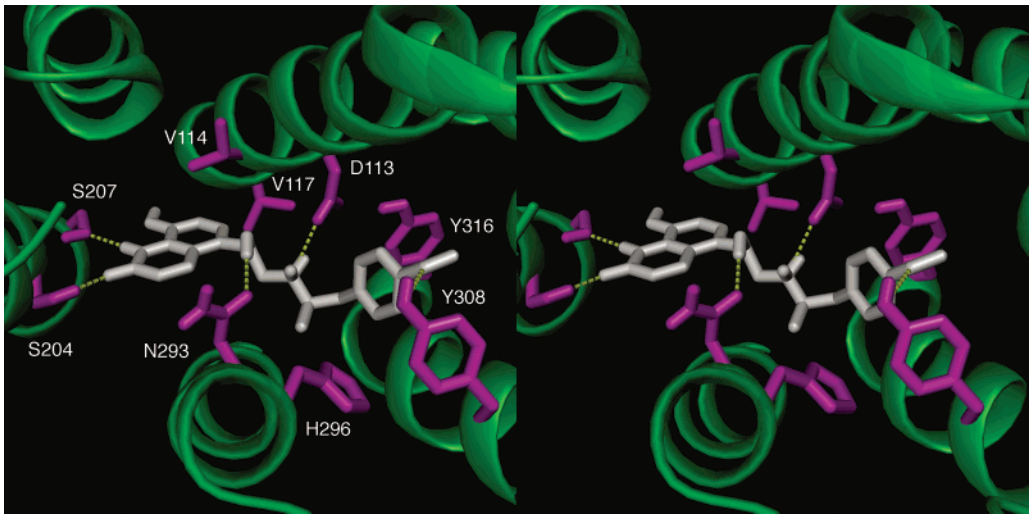

Figure 5. Top (extracellular) stereoview of the complex of β_2-selective ligand, TA-2005, with the de novo model. The ligand is displayed in white, and key binding site residues are shown in magenta. Hydrogen bonds are indicated by dashed yellow lines. Key contacts include a charge-reinforced hydrogen bond between the protonated amine and D113 in TM3, hydrogen bonds between the oxoquinoline ring system of the ligand with S204 and S207 in TM5 and between ligand side chain hydroxyl and N293 in TM6, and an interaction between the *p*-methoxy N-substituent and Y308 at the top of TM7, as well as H296 in TM6 and Y316 in TM7.

additional contact with V117 (TM3) on the floor of the pocket. The chromophore carbonyl accepted a hydrogen bond from S204, while the ring nitrogen donated a hydrogen bond to S207. The larger *p*-methoxyphenyl N-substituent lies just below the conserved disulfide bond in a pocket formed by TM3, TM6, and TM7, where it stacks nicely with Y308, N312, and Y316 in TM7, forming additional contacts with F289, V292, and H296 in TM6 and W109 in TM3. The β-OH group forms a stereoselective hydrogen bond with N293, as observed for small agonists. The ether oxygen can potentially accept a hydrogen bond from Y308. This large agonist cannot fit into the binding pocket present in the β_2-receptor homology model, due to serious steric overlap with residues in the second extracellular loop, as well as W109 in TM3 (Figure 2B).

Antagonists. Antagonist complexes for AmF and *p*BABC are shown in Figures 6 and 7. The de novo β_2-receptor model accommodates the antagonists well in the binding site, and residue N293 forms a stereoselective hydrogen bond with each ligand. Both residues Y199 in TM5 and H93 in TM2 are accessible to the binding pocket. These residues are documented sites of covalent attachment in affinity labeling experiments.[22,23] The aromatic ring system of each antagonist shifts up in the binding pocket 1−2 Å during refinement, close to residue Y199, where they form good aromatic stacking interactions with this and surrounding residues. This positioning of the chromophore is consistent with previous photoaffinity labeling studies for AmF, which forms a covalent bond with the β-carbon of Y199 via a free radical bond insertion mechanism.[22] This shift of the antagonists slightly higher in the ligand-binding pocket separates them from the aromatic wall in TM6 and, to some extent, the S204/S207 pair in TM5, both

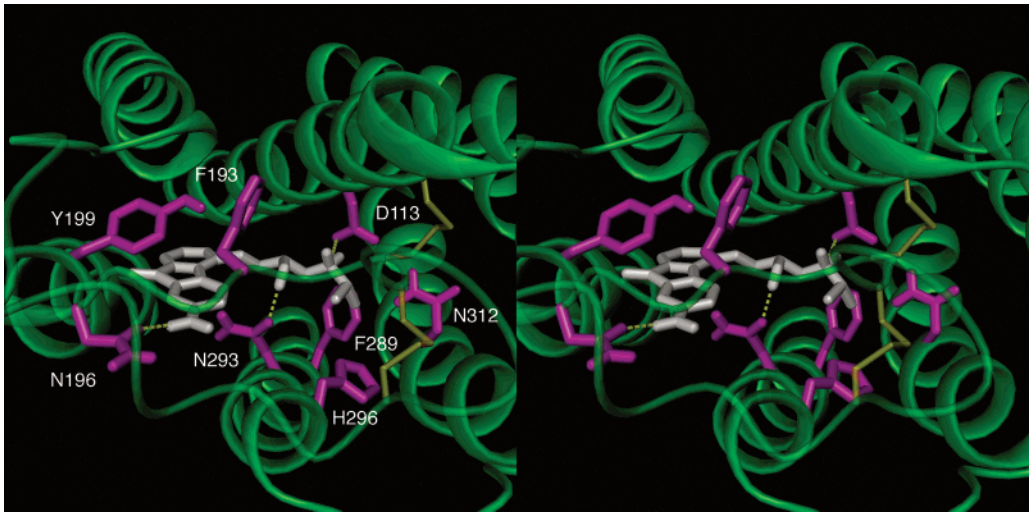

Figure 6. Top (extracellular) stereoview of the complex of photolabile antagonist aminoflisopolol with the de novo β_2-AR model. The ligand is displayed in white, with key active site residues shown in magenta. Y199 in TM5 is the site of covalent attachment in photoaffinity labeling experiments. Other key contacts include a charge-reinforced hydrogen bond between the protonated amine and D113 in TM3 and a hydrogen bond between the ligand side-chain hydroxyl and N293 in TM6, both indicated by dashed yellow lines. N312 in TM7, along with F289 and H296 in TM6, interact with the isopropyl N-substituent. For this complex, the second extracellular loop is included, with the two disulfide bonds highlighted in yellow and loop residue F193 shown interacting with the fluorenone ring of the ligand.

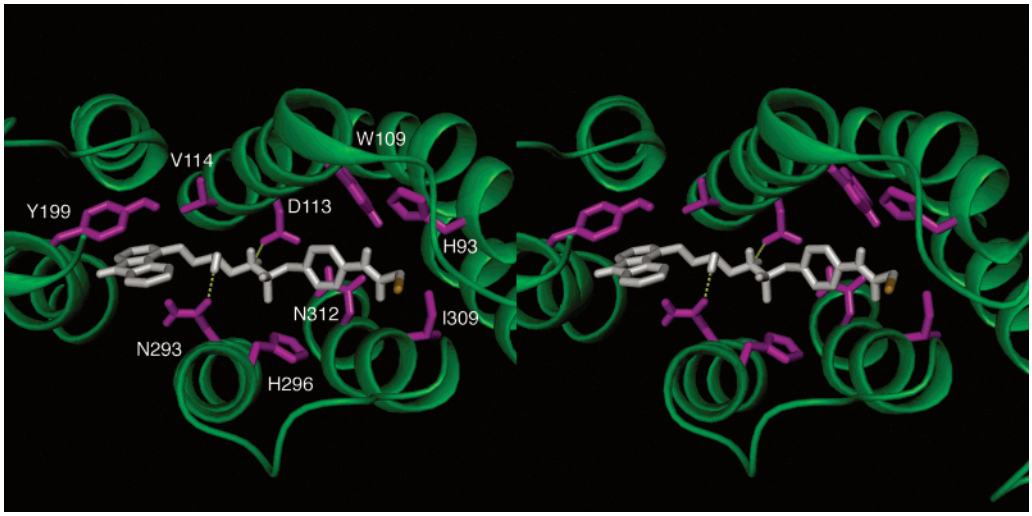

Figure 7. Top (extracellular) stereoview of the complex of antagonist and affinity label, *p*BABcarazolol with the de novo β_2-AR model. The ligand is displayed in white, with bromine highlighted in orange. Key active site residues, shown in magenta, include H93 in TM2, the proposed site of covalent insertion for the N-substituent of *p*BABC, along with Y199 in TM5. Other key contacts include a charge-reinforced hydrogen bond between the protonated amine and D113 in TM3 and a hydrogen bond between the ligand side-chain hydroxyl and N293 in TM6, both indicated by dashed yellow lines. I309 and N312 in TM7 make van der Waals contact with the *p*-bromoacetamido N-substituent, as does W109 in TM3.

of which have been proposed to be involved in conformational changes that accompany receptor activation.[31]

The complex with AmF (Figure 6) is typical of the antagonist complexes. The AmF ring system interacts with residue P168 in TM4, Y199 and A200 in TM5, V297 in TM6, and F193, which is part of the short tether in ECL2 between the conserved disulfide bond to TM3 (C106−C191) and the top of TM5. The propanolamine backbone interacts with V114 and T110 in TM3, while the *N*-isopropyl group interacts with F289 and H296 in TM6, and N312 in TM7. The ring chromophore and propanolamine backbone interactions are essentially identical for the complexes with propranolol and *p*BABC, except near the *N*-alkyl side chain. In the propranolol complex, the *N*-isopropyl group interacts with residue V117 in TM3 and W286, F289, and the alkyl side chain of N293 in TM6. The carazolol derivative *p*BABC was shown previously to label nucleophilic residues in the extracellular end of TM2,[23] and H93 is the prime target residue in TM2. In the model complex, the *p*-bromoacetamidylbenzyl group sits just below the conserved C106−C191 disulfide bond, in a hydrophobic pocket formed by residues W109 in TM3, H296 in TM6, and Y308, I309, and N312 in TM7. In this orientation, the *p*BABC molecule is well positioned for nucleophilic attack by H93, consistent with experimental results (Figure 7). As was observed for larger agonists, large antagonists like AmF and *p*BABC cannot be accommodated in the homology model, due to serious steric conflicts with the second extracellular loop residues as well as W109 in TM3. However, physically plausible

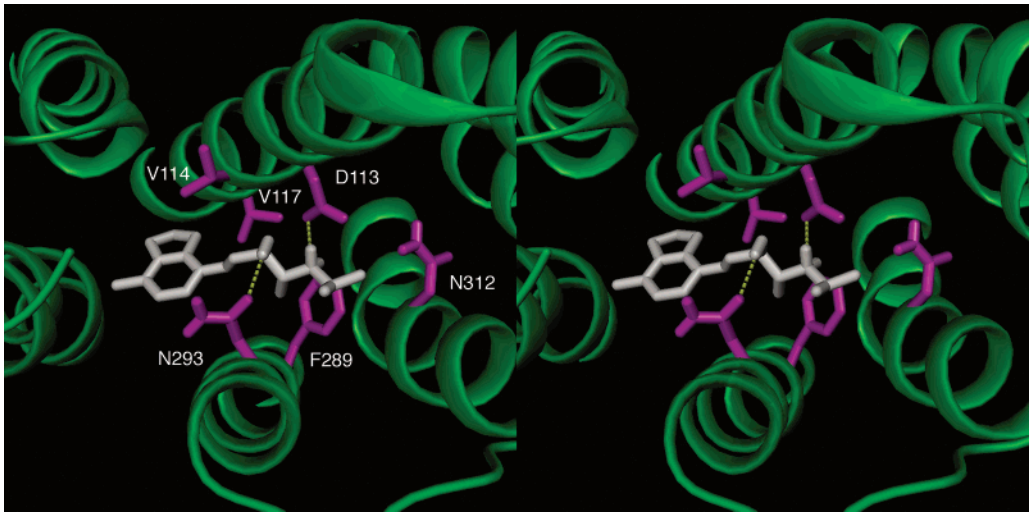

Figure 8. Top (extracellular) stereoview of the complex of inverse agonist ICI-118,551 with the de novo β_2-AR model. The ligand is displayed in white, with key active site residues shown in magenta. Shown here are a charge-reinforced hydrogen bond between the protonated amine and D113 in TM3 and a hydrogen bond between the ligand side-chain hydroxyl and N293 in TM6, both indicated by dashed yellow lines. The ligand also makes van der Waals contact with V114 and V117 in TM3, F289 in TM6, and to a lesser extent N312 in TM7.

complexes can be generated for both the de novo and the homology models with the smaller antagonist propranolol.

In the de novo model antagonist complexes, N293 from TM6 again forms the stereoselective hydrogen bond with each ligand. While N293 is well established as the key hydrogen-bonding partner responsible for stereoselectivity for many agonists, there are no clear experimental data to support a role for this residue in antagonist binding. It has been proposed that stereoselective binding of aryloxypropanolamine antagonists may be determined by a different residue, N312 in TM7.[32] Mutation of N312 in the β_2-receptor reduces dramatically the binding of antagonists like propranolol,[33] and mutation of the equivalent residue in the human serotonin 5-HT_{1A} receptor eliminated stereoselective binding of β-antagonists.[34] However, N312 mutations in the β_2-receptor also reduce agonist binding measurably, and appear to alter contacts with residues in TM1 and TM2.[33,35] On the basis of these results, it seems possible that the deleterious ligand-binding effects produced by N312 mutations in the β_2-receptor may be due, at least in part, to structural perturbations, rather than the simple presence or absence of a ligand contact with residue N312. Residue N312 is oriented toward the ligand-binding pocket in our de novo models, and even makes van der Waals contacts with the antagonist *N*-alkyl groups in many of the complexes. However, N312 is too far removed from the side-chain hydroxyl group in these ligands to form a hydrogen bond. Since AmF covalently labels residue Y199 at the opposite end of the antagonist-binding pocket, this constraint precludes a shift of the ligand to form a hydrogen bond with N312. Instead, a significant shift or tilt of TM7 (~1−2 Å) in our models, with compensatory adjustments of TM1 and TM2, would be necessary to reposition N312 so as to form this proposed hydrogen bond. Our de novo models also suggest other potential hydrogen-bonding partners for the side-chain hydroxyl in antagonist ligands, including T110, D192, or Y308, but there are no experimental data at present to indicate that any of these residues play a role in stereoselective binding of antagonists. These modeling results most likely indicate that the antagonists bind to receptor conformations that are notably different than those represented by either our current de novo receptor models or the homology model, and additional experimental studies to probe antagonist−receptor contacts in greater detail are needed to guide further refinement of antagonist−receptor complexes.

Inverse Agonist. The receptor complex with inverse agonist ICI-118,551 is shown in Figure 8. This molecule shares the phenylpropanolamine side-chain structure present in propranolol and was placed initially in the binding pocket with a similar orientation. There is little specific experimental data available to assess details of the ligand−receptor interaction for ICI-118,551, but the modeling results do indicate that this compound can be accommodated sensibly in both the de novo and homology receptor models, as is also true for propranolol. This is due, in part, to the relatively small size of both ligands, and also to the lack of multiple, specific interactions with the receptor that constrain the exact location or orientation of these ligands. Interestingly, propranolol has been reported to exhibit inverse agonist activity in some assays,[36] so it is perhaps significant that both ICI-118,551 and propranolol can be accommodated well in the homology model, which should presumably be a good reference structure for inverse agonist complexes.

***β*-Receptor Subtype Selectivity.** In an effort to explore the basis of β-receptor subtype selectivity in greater detail, we generated β_1- and β_3-adrenergic receptor models, using the de novo β_2 receptor model as a template. The high sequence similarity for these receptors, particularly in the transmembrane helical bundle domain (69% sequence identity and 87% identity plus conservative substitution for β_1 versus β_2; 65% identity and 87% identity plus conservative substitution for β_1 versus β_3; 60% identity and 83% identity plus conservative substitution for β_2 versus β_3), suggests that they must possess quite similar three-dimensional structures. The residues lining the binding site region of the three receptors are nearly identical (75−85%

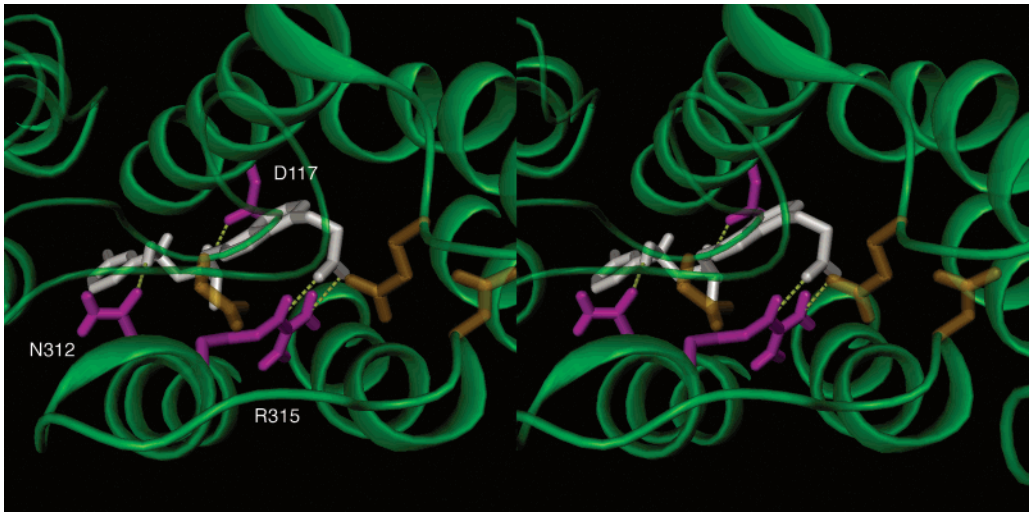

Figure 9. Top (extracellular) stereoview of the complex of β_3-selective ligand, AJ-9677, with the de novo β_3-AR model. The ligand is displayed in white, and key binding site residues are shown in magenta. Hydrogen bonds are indicated by dashed yellow lines. Key contacts include a charge-reinforced hydrogen bond between the protonated amine and D117 in TM3 (homologous to D113 in the β_2-receptor), a hydrogen bond between the ligand side-chain hydroxyl and N312 in TM6 (homologous to N293 in β_2-receptor), and a charge-reinforced bifurcated hydrogen bond between the carboxyl group of the N-substituent and R315 at the top of TM6. Two acidic residues are located near this region of the ligand-binding site in β_1-AR (E125 and D356, shown in orange), but are not present in β_2- or β_3-receptors. A third acidic residue, found in both β_1-AR (D217, shown in orange) and β_2 (D192), but not β_3-receptors, is located in the second extracellular loop adjacent to the disulfide bond to TM3. The second extracellular loop is as shown in Figure 5, but the two disulfide bonds have been omitted for clarity.

sequence identity and 95−100% identity plus conservative substitution), so the binding site pockets in each receptor subtype must also have extremely similar structures and hydration characteristics. The most notable difference for the three receptor subtypes is a residue in TM6 located just above the binding site in our models, one turn above N293 and oriented toward the *N*-substituent of bound ligands. This residue is a histidine in β_2 (H296), a lysine in β_1 (K347), and an arginine in β_3-receptor (R315). These three residues differ substantially in size, possible charge state (in the case of H296), and the number and orientation of hydrogen bonds they can form with neighboring residues or ligands.

The molecule TA-2005 (Figure 3C) has been proposed to be a β_2-selective ligand, with selectivity ratios of ∼50 and ∼150 for β_2- vs β_1- and β_3-receptors, respectively.[37,38] Through ligand-binding measurements for a number of β-receptor chimeras and site-directed mutants, Kikkawa et al. have determined that a single residue, Y308 in the extracellular end of TM7 in the β_2-receptor, is responsible for β-receptor subtype selectivity for TA-2005.[39] This residue is a phenylalanine in β_1 and β_3-receptors. In our β_2-receptor model, Y308 is positioned directly above the binding site, and is involved in a hydrogen bond to D192 in the second extracellular loop, adjacent to the conserved disulfide bond to TM3. After structural refinement of the β_1-receptor model with low-temperature molecular dynamics, the phenylalanine at this position shifts toward the bilayer, since it cannot form a hydrogen bond with the second extracellular loop. Interestingly, Kikkawa et al. have proposed that some structural change is induced by the introduction of a hydrogen-bonding mutant at this position in the β_1-receptor (F359Y).[38] When we manually docked TA-2005 in our de novo β_2-receptor model, imposing key receptor−ligand contacts with D113, S204, and S207, the N-substituent of the ligand (*p*-methoxyphenyl) interacted directly with Y308 and H296 in TM6, and the hydroxyl group of Y308 can potentially form a hydrogen bond with the *p*-methoxy oxygen of the ligand (Figure 5). This model suggests that H296 might also have an impact on subtype selectivity. The larger lysine or arginine residues at this position in β_1- and β_3-receptors would potentially cause considerable steric conflict with the *p*-methoxyphenyl substituent in TA-2005.

Despite the extremely high sequence similarity for all three receptor subtypes, there is emerging evidence that the β_3-adrenergic receptor may bind ligands somewhat differently than β_1- and β_2-receptors. A number of ligands that behave as antagonists for β_1- and β_2-receptors are full agonists for the β_3-receptor.[40] Additionally, a number of ligands which exhibit impressive β_3-receptor selectivity have been developed, confirming that exploitable differences do exist between these receptors.[24] Most β_3-selective agonists do not share epinephrine's catechol ring, but instead have a pyrimidine or *m*-chlorobenzyl ring, or in some cases a more extensive heteroaromatic ring system reminiscent of β-receptor antagonists. One interesting β_3-receptor agonist is AJ-9677.[41] This molecule has a nanomolar EC_{50} for β_1- and β_2-receptors (6.4 and 13 nM, respectively), but is 100−200 times more potent for human β_3-receptor (EC_{50} = 0.062 nM).[24] AJ-9677 (Figure 3D) contains an unusual indol-7-yloxy acetic acid substituent on the secondary nitrogen atom that could be partially responsible for the observed selectivity. At physiological pH, this N-substituent would be ionized, resulting in a bulky, negatively charged fragment that the receptor must accommodate. To explore the potential receptor interactions, a geometry-optimized conformation of AJ-9677 was docked in all three β-receptor subtype models, with the protonated amine positioned near D113 and the *m*-chlorobenzyl ring near the aromatic wall on TM6. In the β_3-receptor model, this docking orientation places the N-substituent at the top of the binding site, between

TM3, TM6, and TM7, where the ligand carboxylate group forms a charge-reinforced, bifurcated hydrogen bond with R315 (Figure 9). In the β_2-receptor model, the analogous docking places the carboxylate of AJ-9677 between the β-carbon of Y308 and the disulfide bond in the extracellular region. The closest basic residue, K305 at the top of TM7, is too distant and not optimally oriented to interact with the ligand. Residue H296 in TM6 is not favorably positioned to form a strong interaction with the ligand carboxylate, even in the event that this residue is fully protonated. Additionally, β_3 residue A197, the position immediately following the conserved disulfide bond in the extracellular domain of the β-receptors, is an aspartate in β_1 (D217) and β_2 (D192). This section of the second extracellular loop is relatively conformationally constrained, as there are only five residues between the disulfide cross link to TM3 and the top of TM5, as discussed above. The proximity of this acidic residue, combined with the lack of a compelling basic charge partner for the ligand carboxylate, suggests a possible basis for the lower affinity of this drug for β_1- and β_2- versus β_3-receptors. In the β_1-receptor model, residue K347 in TM6 can interact with the ligand carboxylate group, but only a single charge-reinforced hydrogen bond can be formed. However, in the β_1-receptor, there are two additional acidic residues nearby, E125 in the first extracellular loop and D356 at the top of TM7, which could partially destabilize the complex (Figure 9). There are no acidic residues at comparable loop positions in the β_2- or β_3-receptors.

AJ-9677 binds well to all three subtypes, but binds particularly well to the β_3-receptor. The receptor subtype-specific sequence variation in TM6 discussed here suggests a possible explanation. The arginine found in the β_3-receptor (R315) can form a much stronger interaction with the acidic moiety of the bound ligand than the lysine (K347) or histidine (H296) found in β_1- and β_2-receptors, respectively. Many of the promising new β_3-selective ligands contain an N-substituent with either a carboxylate or a sulfonamide functional group.[24] Thus, it is possible that a key interaction with R315 in the β_3-adrenergic receptor can explain the dramatic β_3 selectivity of these compounds.

Conclusions

Our results, together with earlier studies, strongly support the idea that the current rhodopsin crystal structure is probably not an optimal structural template for homology modeling of GPCR−agonist or neutral antagonist complexes. Since the rhodopsin crystal structure reflects an inactive conformation, this conclusion is neither surprising nor radical. It was noted previously that 11-*cis*-retinal functions as a potent inverse agonist in the rhodopsin structure,[12,42] so it is unreasonable to expect that the current rhodopsin crystal structure can be used, without conformational modification, to generate good models for GPCR−agonist complexes. Both the de novo and homology models can accommodate the inverse agonist ICI-118,551 quite sensibly, which is expected, since the rhodopsin crystal structure should serve as a good homology template for inverse agonist complexes. Both models also accommodate the antagonist propranolol quite well. As noted above, it is quite interesting that propranolol is also classified as an inverse agonist in some activity assays. Small agonists, like epinephrine or isoproterenol, can be accommodated in the strict homology model modestly well, but the key stereoselective hydrogen bond with N293 in TM6 cannot be formed in the homology model. We suspect that these ligands do not pose particularly stringent challenges for model assessment at any rate, since both epinephrine and isoproterenol have been incorporated successfully in a large number of quite diverse β-adrenergic receptor models over the years. Larger agonists and neutral antagonists pose far greater challenges in docking exercises. Our de novo models, refined using numerous ligand contacts as structural constraints, appear to better explain details of receptor−agonist interactions. Unlike the strict rhodopsin homology models, our de novo models can accommodate a wide variety of ligands as suggested by experimental studies. Although not imposed as a constraint in model-building and ligand-docking exercises, the de novo models suggest that residue N293 in TM6 is primarily responsible for stereoselective agonist binding, as supported by experimental studies. The de novo models also provide interesting and testable hypotheses for β-receptor subtype ligand-binding selectivity for a number of β_2- and β_3-selective ligands. None of the models provides a completely satisfactory explanation for stereoselective binding of β-adrenergic antagonists, although they suggest a number of possible alternatives that may warrant further experimental testing. It is likely that antagonists bind preferentially to receptor conformations that differ in important details from either our de novo or homology receptor models, and further experimental studies for β-receptor-antagonist complexes would facilitate future modeling studies.

The de novo models share many structural features with the rhodopsin crystal structure. The most notable differences are localized in regions where significant changes would be expected logically, such as the extracellular loop conformations, and the exact orientation and positioning of TM6. It is quite intriguing that, with the exception of extracellular loop conformations, the most notable difference between our de novo and homology models is the exact tilt and orientation of TM6. Other recent models for GPCR−agonist complexes also indicate significant changes in TM6 positioning relative to the rhodopsin crystal structure, and experimental studies for both rhodopsin[14] and β_2-adrenergic receptor[43] suggest that a rotation and/or tilt of TM6 appears to accompany agonist activation in these GPCRs. In our de novo models with agonists, it is precisely a rotation and tilt of TM6 that enables formation of the stereoselective hydrogen bond between N293 and the ligand hydroxyl group attached to the side-chain chiral carbon.

At present, it is not possible to define a reasonable reaction coordinate to model the conformational transition from the rhodopsin crystal structure conformation (i.e., the inactive conformation) to our proposed "active" conformation for the β-adrenergic receptors, due to the complexity of the numerous, coupled local conformational changes that must occur. However, comparison of our models for the "active" and "inactive" conformational states does not reveal any structural features in the β-adrenergic receptors that would hinder or preclude

this conformational change. It is unlikely that this conformational transition would occur spontaneously in equilibrium molecular dynamics simulations using current state-of-the-art approaches. Therefore, additional experimental data will be needed to help define plausible pathways for the conformational change, which may then be modeled using steered molecular dynamics simulations or a similar technique. For the rhodopsin/11-*cis*-retinal complex, an approximate reaction coordinate for the conformational transition might be based successfully on a forced transition for 11-*cis*-retinal to *all-trans*-retinal in the rhodopsin-binding pocket.

There appears to be no simple, consistent explanation for ligand stereoselectivity for β-adrenergic agonists and antagonists. This strongly suggests that a single, static three-dimensional model is not adequate to explain stereoselective ligand binding (or other ligand-binding characteristics) for all adrenergic ligands. This is quite consistent with the idea that GPCRs undergo facile transitions between multiple conformational states under normal conditions,[18] and that agonists, neutral antagonists, and inverse agonists preferentially bind and stabilize different receptor conformations.[17,44] If true, this also suggests that many independent ligand−receptor complex structures must be solved before we will understand fully the details of receptor subtype-selective ligand binding.

In summary, we have presented here three-dimensional models for a number of agonist and antagonist complexes with β-adrenergic receptors that are consistent with a large body of experimental data, and these models lead us to propose experimentally testable hypotheses for the molecular bases of β-receptor agonist subtype selectivity and antagonist stereoselectivity. As more data are available to better characterize the details of β-receptor complexes with these ligands, we will be able to resolve these issues more definitively.

Experimental Section

Homology models for the β_2-adrenergic receptor were based directly on the rhodopsin crystal structure (1F88) backbone conformation, with amino acid side-chain replacement to generate the β_2-receptor sequence. Side-chain conformations were selected so as to minimize steric repulsion with neighboring side chains, using the automated side-chain placement program SCRWL,[45] together with manual adjustment when necessary, and a standard amino acid rotamer library.[46] The resultant structure was refined with limited conjugate gradient energy minimization and low-temperature (20 K) molecular dynamics to relieve remaining unfavorable steric interactions in the helix bundle. The AMBER 7.0 package[47] was used for all energy minimization and molecular dynamics calculations, with the standard AMBER94 all-atom potential energy functions.[48] The programs PROCHECK[49] and QPACK[50] were used to assess the structural integrity (e.g., backbone and side-chain torsion angles, stereochemical constraints, side-chain packing interactions, and hydrogen bond donor−acceptor interactions) for the homology model.

All de novo models for the β-adrenergic receptors were constructed using the interactive molecular graphics program PSSHOW.[51] Helix bundle models from earlier β_2-receptor modeling studies[6] were used as starting structures, and the tilt angle, longitudinal shift, and rotation about the helix axis were adjusted for each individual helix to provide better agreement with recent experimental data regarding localization of certain amino acid residues in the ligand-binding site. The resultant structures were checked for bad side-chain steric interactions, and any necessary adjustments were made using an automated side-chain rotamer search procedure within PSSHOW, based on a standard rotamer library.[46] Extracellular and cytosolic loop segments were generated using an automated procedure reported previously.[11] Briefly, peptide segments corresponding to the amino- and carboxy-terminal halves of each loop were constructed in extended conformation and attached to the ends of the appropriate transmembrane helices. Weak harmonic constraints were then applied gradually during the course of short (10−20 ps), low-temperature (35 K) molecular dynamics simulations to close the loop segments, forming a trans amide bond at the ligation site. For extracellular loops containing the disulfide cross links, the loops were generated simultaneously, with constraints to ligate each loop as well as close both disulfide bonds. This protocol avoids the introduction of unfavorable steric interactions during the loop generation procedure, while maintaining energetically allowable peptide backbone and side-chain conformations. The modified helix bundle structures were then refined with limited energy minimization and low-temperature molecular dynamics as described above for homology models. The β_1- and β_3-receptors were generated directly from the refined β_2 template, as only a few amino acid side-chain substitutions were necessary to create β_1- and β_3-receptor sequences. Finally, the β_1- and β_3-receptor models were refined with limited energy minimization and molecular dynamics to remove any residual bad steric interactions. All de novo models were also evaluated for structural integrity using PROCHECK[49] and QPACK.[50]

Epinephrine was then docked manually into the binding pocket for each model, and the complex was refined, using a 20-ps, low-temperature (5 K) molecular dynamics simulation with a distance-dependent dielectric constant in vacuo, including 1.0 kcal mol^{-1} Å^{-1} harmonic restraints on the backbone atoms of the transmembrane helices and 5.0 kcal mol^{-1} Å^{-1} restraints on key ligand−receptor contacts. Helix side chains and loops were allowed to move freely during the initial refinement phase. In a second phase, the epinephrine position restraints were removed and the complex was relaxed during an additional 10-ps molecular dynamics simulation. The refined epinephrine complex was then used as a starting structure for all other ligand complexes, after removal of epinephrine from the ligand-binding pocket.

Extensive conformational searches were performed for the ligands, so that we could consider all low-energy conformations in subsequent rigid molecule manual and automated ligand-docking exercises. Several conformational search methods were used, including systematic search and hybrid Monte Carlo search for all rotatable bonds, and a simulated annealing protocol. The hybrid Monte Carlo search was performed using the MOE package,[52] with an MD/MC ratio of 4 and a 0.005-ps dynamics time step at 300 K, yielding 5000 conformers per run. Each conformer was then energy minimized, and a pair RMSD cutoff criterion of 1−2 Å was used to eliminate redundant conformers.

In the simulated annealing protocol, a generalized Born continuum solvation model incorporated in the AMBER package was used to reduce the dominating effect of the electrostatic interactions between the charged, protonated amine and polar substituents such as hydroxyl groups. Without the charge screening effect of the generalized Born model, the electrostatic interactions with the protonated amine tended to heavily bias sampling in favor of compact, folded conformers with extensive intramolecular hydrogen bonding. During the simulated annealing procedure, ligands were heated from 10 to 1200 K, and then slowly cooled in stages. The heating/annealing cycle was repeated 30−50 times for each ligand in order to generate an ensemble of conformations, which were then minimized to 0.01 kcal mol^{-1} Å^{-1} RMSD using a Newton−Rhapson algorithm. The ensembles were then clustered using the Compare program,[53] and all conformations within 3 kcal/mol of the global minimum were chosen for docking exercises. A 10 kcal/mol energy cutoff was used in *p*BABC conformational searches, as no alternate conformations were discovered within 6 kcal/mol of the global minimum for this ligand. The sampling

protocols used in this study may likely exaggerate the energetic penalty for extended versus compact, folded conformations (e.g., the global minimum) for *p*BABC. However, we wanted to generate a collection of extended *p*BABC conformations for subsequent docking exercises, since experimental data suggest that the receptor-bound conformation must be extended.

Low-energy conformers of each ligand were then docked in the β_2-receptor model, using both manual and automated docking techniques. For each complex, key ligand−receptor contacts inferred from experimental studies were maintained (e.g., protonated amine/D113 counterion interactions, catechol hydrogen bonds, etc.). Adjustments to the receptor to accommodate any particular ligand were restricted to isolated amino acid side-chain rotations in the binding site region, and rotations were further restricted to allowable rotamers.[46] After docking, limited energy minimization and unrestrained, low-temperature (5 K) molecular dynamics were used to relieve any residual bad steric contacts. The final docked complexes were examined to ensure the receptor model still possessed sensible side-chain conformations and packing interactions as described previously. The quality of ligand−receptor interactions was assessed for steric, charge−charge, and hydrogen-bonding interactions. Hydrogen bonds were considered "good" if donor−acceptor distances were ∼2.8−3.2 Å and the solid cone angle formed by donor atom−hydrogen vector with the donor atom−acceptor atom vector was ∼0.0 ± 20°.

Standard AMBER all-atom potential functions were used for all ligands.[48] The antagonists aminoflisopolol (AmF) and *p*-(bromoacetamidyl)benzylcarazolol (*p*BABC) required the definition of two new atom types and the addition of some parameters to the standard AMBER parm94 data set. The heteroaromatic ring nitrogen in *p*BABC was assigned atom type "NZ" and directly bonded carbons, atom type "CZ". These new atom types have close analogues in the purine nucleic acids bases, so bond, bond angle, and torsion parameters were taken from the purine parameters, with equilibrium bond lengths and angles modified slightly on the basis of the ligand-optimized geometries (Supporting Information).

Ligand geometry optimization was performed with Gaussian 98,[54] using restricted Hartree−Fock calculations and a 3/21G basis set, while partial charges for all ligands were derived from ab initio electrostatic potential calculations with a 6-31G* basis set. Final partial charges were fitted using the RESP program.[55] Manual model construction, ligand docking, and visual analysis of complexes were performed using PSSHOW and MD-DISPLAY programs.[51,56] The DOCK package was used for all automated rigid docking exercises.[57] Multiple sequence alignment and analyses were performed with the AMPS and AMAS programs.[58]

Acknowledgment. This work was supported in part by grant NS33290 from the National Institutes of Health. K.E.F. was supported by training grant T32 GM08320 from the National Institutes of Health. We thank Dr. Eric Dawson for helpful discussion and technical assistance.

Supporting Information Available: Potential function parameters for all ligands presented here. This material is available free of charge via the Internet at http://pubs.acs.org. Coordinates for all receptor−ligand complexes discussed here are available from the corresponding author upon request.

References

(1) Bikker, J. A.; Trump-Kallmeyer, S.; Humblet, C. G-protein coupled receptors: Models, mutagenesis, and drug design. *J. Med. Chem.* **1998**, *41*, 2911−2927.
(2) Gershengorn, M. C.; Osman, R. Minireview: insights into G protein-coupled receptor function using molecular models. *Endocrinology* **2001**, *142*, 2−10.
(3) Henderson, R.; Baldwin, J. M.; Ceska, T. A.; Zemlin, F.; Beckmann, E.; Downing, K. H. Model for the structure of bacteriorhodopsin based on high-resolution electron cryomicroscopy. *J. Mol. Biol.* **1995**, *213*, 899−929.
(4) Pebay-Peyroula, E.; Rummel, G.; Rosenbusch, J. P.; Landau, E. M. X-ray structure of bacteriorhodopsin at 2.5 angstroms from microcrystals grown in lipidic cubic phases. *Science* **1997**, *277*, 1676−1681.
(5) Soppa, J. Two hypotheses—one answer: Sequence comparison does not support an evolutionary link between halobacterial retinal proteins including bacteriorhodopsin and eukaryotic G-protein-coupled receptors. *FEBS Lett.* **1994**, *342*, 7−11.
(6) Kontoyianni, M.; DeWeese, C.; Penzotti, J. E.; Lybrand, T. P. Three-dimensional models for agonist and antagonist complexes with b_2 adrenergic receptor. *J. Med. Chem.* **1996**, *39*, 4406−4420.
(7) Palczewski, K.; Kumasaka, T.; Hori, T.; Behnke, C. A.; Motoshima, H.; Fox, B. A.; Trong, I. L.; Teller, D. C.; Okada, T.; Stenkamp, R. E.; Yamamoto, M.; Miyano, M. Crystal Structure of Rhodopsin: A G Protein-Coupled Receptor. *Science* **2000**, *289*, 739−745.
(8) Bissantz, C.; Bernard, P.; Hibert, M.; Rognan, D. Protein-based virtual screening of chemical databases. II. Are homology models of G-protein coupled receptors suitable targets? *Proteins: Struct.. Funct. Genet.* **2003**, *50*, 5−25.
(9) Archer, E.; Maigret, B.; Escrieut, C.; Pradayrol. L.; Fourmy, D. Rhodopsin crystal: New template yielding realistic models of G-protein-coupled receptors? *Trends Pharmacol. Sci.* **2003**, *24*, 36−40.
(10) Chambers, J. J.; Nichols, D. E. A homology-based model of the human 5-HT_{2A} receptor derived from an *in silico* activated G-protein coupled receptor. *J. Comput.-Aided Mol. Des.* **2002**, *16*, 511−520.
(11) Ding, X.-Q.; Pinon, D. I.; Furse, K. E.; Lybrand, T. P.; Miller, L. J. Refinement of the conformation of a critical region of charge−charge interaction between cholecystokinin and its receptor. *Mol. Pharmacol.* **2002**, *61*, 1041−1052.
(12) Okada, T.; Ernst, O. P.; Palczewski, K.; Hofmann, K. P. Activation of rhodopsin: new insights from structural and biochemical studies. *Trends Biochem. Sci.* **2001**, *26*, 318−324.
(13) Farrens, D. L.; Altenbach, C.; Yang, K.; Hubbell, W. L.; Khorana, H. G. Requirement of rigid-body motion of transmembrane helices for light activation of rhodopsin. *Science* **1996**, *274*, 768−770.
(14) Dunham, T. D.; Farrens, D. L. Conformational changes in rhodopsin- Movement of helix F detected by site-specific chemical labeling and fluorescence spectroscopy. *J. Biol. Chem.* **1999**, *274*, 1683−1690.
(15) Altenbach, C.; Cai, K. W.; Klein-Seetharaman, J.; Khorana, H. G.; Hubbell, W. L. Structure and function in rhodopsin: Mapping light-dependent changes in the distance between residue 65 in helix TM1 and residues in the sequence 306−319 at the cytoplasmic end of helix TM7 and in helix H8. *Biochemistry* **2001**, *40*, 15483−15492.
(16) Ghanouni, P.; Gryczynski, Z.; Steenhuis, J. J.; Lee, T. W.; Farrens, D. L.; Lakowicz, J. R.; Kobilka, B. K. Functionally different agonists induce distrinct conformations in the G protein coupling domain of the beta(2) adrenergic receptor. *J. Biol. Chem.* **2001**, *276*, 24433−24436.
(17) Peleg, G.; Ghanouni, P.; Kobilka, B. K.; Zare, R. N. Single-molecule spectroscopy of the beta(2) adrenergic receptor: Observation of conformational substates in a membrane protein. *Proc. Natl. Acad. Sci. U.S.A.* **2001**, *98*, 8469−8474.
(18) Kenakin, T. Agonist-specific receptor conformations. *Trends Pharm. Sci.* **1997**, *18*, 416−417.
(19) Unger, V. M.; Hargrave, P. A.; Baldwin, J. M.; Schertler, G. F. X. Arrangement of rhodopsin transmembrane α-helices. *Nature* **1997**, *389*, 203−206.
(20) Dixon, R. A. F.; Sigal, I. S.; Strader, C. D. Structure−function analysis of the β-adrenergic receptor. *Cold Spring Harbor Symp. Quantum Biol.* **1988**, *53*, 487−497.
(21) Strader, C. D.; Candelore, M. R.; Hill, W. S.; Sigal, I. S.; Dixon, R. A. F. Identification of Two Serine Residues Involved in Agonist Activation of the β-Adrenergic Receptor. *J. Biol. Chem.* **1989**, *264*, 13572−13578.
(22) Wu, Z.; Thiriot, D. S.; Ruoho, A. E. Tyr199 in transmembrane domain 5 of the b2-adrenergic receptor interacts directly with the pharmacophore of a unique fluorenone-based antagonist. *Biochem. J.* **2001**, *354*, 485−491.
(23) Dohlman, H. G.; Caron, M. G.; Strader, C. D.; Amlaiky, N.; Lefkowitz, R. J. Identification and Sequence of a Binding Site Peptide of the b_2-adrenergic Receptor. *Biochemistry* **1988**, *27*, 1813−1817.
(24) de Souza, C. J.; Burkey, B. F. Beta(3)-adrenoceptor agonists as anti-diabetic and anti-obesity drugs in humans. *Curr. Pharmceut. Des.* **2001**, *7*, 1433−1449.
(25) MaloneyHuss, K.; Lybrand, T. P. Three-dimensional structure for the b_2 adrenergic receptor protein based on computer modeling studies. *J. Mol. Biol.* **1992**, *225*, 859−871.
(26) Sansom, M. S. P.; Weinstein, H. Hinges, swivels, and switches: The role of prolines in signaling via transmembrane alpha-helices. *Trends Pharmacol. Sci.* **2000**, *21*, 445−451.

(27) Sankararamakrishnan, R.; Vishveshwara, S. Geometry of proline-containing alpha-helices in proteins. *Int. J. Pept. Protein Res.* **1992**, *39*, 356−363.
(28) Liapakis, G.; Ballesteros, J. A.; Papachristou, S.; Chan, W. C.; Chen, X.; Javitch, J. A. The forgotten serine. A critical role for Ser-203 (5.42) in ligand binding to and activation of the b2-adrenergic receptor. *J. Biol. Chem.* **2000**, *275*, 37779−37788.
(29) Dohlman, H. G.; Caron, M. G.; DeBlasi, A.; Frielle, T.; Lefkowitz, R. J. Role of Extracellular Disulfide-Bonded Cysteines in the Ligand Binding Function of the Beta(2)-Adrenergic Receptor. *Biochemistry* **1990**, *29*, 2335−2342.
(30) Noda, K.; Saad, Y.; Graham, R. M.; Karnik, S. S. The high affinity state of the beta-2 adrenergic receptor requires unique interaction between conserved and non-conserved extracellular loop cysteines. *J. Bol. Chem.* **1994**, *269*, 6743−6752.
(31) Visiers, I.; Ballesteros, J. A.; Weinstein, H. Three-dimensional representations of G protein-coupled receptor structures and mechanisms. *Methods Enzymol.* **2001**, *343*, 329−371.
(32) Zuurmond H. M.; Hessling J.; Bluml K.; Lohse M.; Ijzerman A. P. Study of interaction between agonists and Asn293 in helix VI of human beta(2)-adrenergic receptor. *Mol. Pharmacol.* **1999**, *56*, 909−16.
(33) Suryanarayana, S.; Kobilka, B. K. Amino acid substitutions at position 312 in the seventh hydrophobic segment of the b2-adrenergic receptor modify ligand-binding specificity. *Mol. Pharmacol.* **1993**, *44*, 111−114.
(34) Kuipers, W.; Link, R.; Standaar, P. J.; Stoit, A. R.; van Wijngaarden, I.; Leurs, R.; Ijzerman, A. P. Study of the interaction between aryloxypropanolamines and Asn 386 in helix VII of the human 5-hydroxytryptamine1A receptor. *Mol. Pharmacol.* **1997**, *51*, 889−896.
(35) Mizobe, T.; Maze, M.; Lam, V.; Suryanarayana, S.; Kobilka, B. K. Arrangement of transmembrane domains in adrenergic receptors. Similarity to bacteriorhodopsin. *J. Biol. Chem.* **1996**, *271*, 2387−2389.
(36) Azzi, M.; Piñeyro, G.; Pontier, S.; Parent, S.; Ansanay, H.; Bouvier, M. Allosteric effects of G protein overexpression on the binding of β-adrenergic ligands with distinct inverse efficacies. *Mol. Pharmacol.* **2001**, *60*, 999−1007.
(37) Kikkawa, H.; Naito, K.; Ikezawa, K. Tracheal relaxing effects and beta2-selectivity of TA-2005, a newly developed bronchodilating agent, in isolated guinea pig tissues. *Jpn. J. Pharm.* **1991**, *57*, 175−85.
(38) Kikkawa, H.; Kurose, H.; Isogaya, M.; Sato, Y.; Nagao, T. Differential contribution of two serine residues of wild type and constitutively active β_2-adrenoceptors to the interaction with β_2-selective agonists. *Br. J. Pharmacol.* **1997**, *121*, 1059−1064.
(39) Kikkawa, H.; Isogaya, M.; Nagao, T.; Kurose, H. The role of the seventh transmembrane region in high affinity binding of a β_2-selective agonist TA-2005. *Mol. Pharmacol.* **1998**, *53*, 128−134.
(40) Blin, N.; Camoin, L.; Maigret, B.; Strosberg, D. A. Structural and conformational features determining selective signal transduction in the Beta(3)-adrenergic receptor. *Mol. Pharmacol.* **1993**, *44*, 1094−1104.
(41) Kato, S.; Harada, H.; Fujii, A.; Kotai, O. Preparation of optically active indoles and their intermediates as antidiabetics and antiobesity agents. *Jpn. Kokai Tokkyo Koho* **1999**, 13 pp.
(42) Rao, V. R.; Oprian, D. D. Activating mutations of rhodopsin and other G protein-coupled receptors. *Annu. Rev. Biophys. Biomol. Struct.* **1996**, *25*, 287−314.
(43) Ghanouni, P.; Steenhuis, J. J.; Farrens, D. L.; Kobilka, B. K. Agonist-induced conformational changes in the G-protein-coupling domain of the β_2 adrenergic receptor. *Proc. Natl. Acad. Sci. U.S.A.* **2001**, *98*, 5997−6002.
(44) Salamon, Z.; Hruby, V. J.; Tollin, G.; Cowell, S. Binding of agonists, antagonists, and inverse agonists to the human delta-opioid receptor produces distinctly different conformational states distinguishable by plasmon-waveguide resonance spectroscopy. *J. Pept. Res.* **2002**, *60*, 322−328.
(45) Bower, M. J.; Cohen, F. E.; Dunbrack Jr., R. L. Prediction of protein side-chain rotamers from a backbone-dependent rotamer library: A new homology modeling tool. *J. Mol. Biol.* **1997**, *267*, 1268−1282.
(46) Dunbrack Jr., R. L.; Karplus, M. Backbone-dependent rotamer library for proteins: Application to side-chain prediction. *J. Mol. Biol.* **1993**, *230*, 543−574.
(47) Pearlman, D. A.; Case, D. A.; Caldwell, J. W.; Ross, W. S.; Cheatham, T. E.; DeBolt, S.; Ferguson, D.; Seibel, G.; Kollman P. A. AMBER, a package of computer programs for applying molecular mechanics, normal mode analysis, molecular dynamics and free energy calculations to simulate the structural and energetic properties of molecules. *Comput. Phys. Commun.* **1995**, *91*, 1−41.
(48) Cornell, W. D.; Cieplak, P.; Bayly, C. I.; Gould, I. R.; Merz, K. M., Jr.; Ferguson, D. M.; Spellmeyer, D. C.; Fox, T.; Caldwell, J. W.; Kollman, P. A. A second generation force field for the simulation of proteins and nucleic acids. *J. Am. Chem. Soc.* **1995**, *117*, 5179−5197.
(49) Laskowski, R. M. M.; Moss D.; Thornton, J. PROCHECK: A program to check the stereochemical quality of protein structures. *J. Appl. Crystallogr.* **1993**, *26*, 283−291.
(50) Gregoret, L. M.; Cohen, F. E. Novel method for the rapid evaluation of packing in protein structures. *J. Mol. Biol.* **1990**, *211*, 959−74.
(51) Swanson, E. *PSSHOW*, Version 2.4; Seattle, WA, 1995.
(52) *Molecular Operating Environment*, 2000.02; Chemical Computing Group Inc.: Montreal, Quebec, Canada, 2000 (http://www.chemcomp.com).
(53) Blaney, J. M.; Dixon, J. S. Distance geometry in molecular modeling. *Rev. Comput. Chem.* **1994**, *5*, 299−335.
(54) Frisch, M. J.; Trucks, G. W.; Schlegel, H. B.; Scuseria, G. E.; Robb, M. A.; Cheeseman, J. R.; Zakrzewski, V. G.; Montgomery, J. A., Jr.; Stratmann, R. E.; Burant, J. C.; Dapprich, S.; Millam, J. M.; Daniels, A. D.; Kudin, K. N.; Strain, M. C.; Farkas, O.; Tomasi, J.; Barone, V.; Cossi, M.; Cammi, R.; Mennucci, B.; Pomelli, C.; Adamo, C.; Clifford, S.; Ochterski, J.; Petersson, G. A.; Ayala, P. Y.; Cui, Q.; Morokuma, K.; Malic, D. K.; Rabuck, A. D.; Raghavachari, K.; Foresman, J. B.; Cioslowski, J.; Ortiz, J. V.; Baboul, A. G.; Stefanov, B. B.; Liu, G.; Liashenko, A.; Piskorz, P.; Komaromi, I.; Gomperts, R.; Martin, R. L.; Fox, D. J.; Keith, T.; Al-Laham, M. A.; Peng, C. Y.; Nanayakkara, A.; Challacombe, M.; Gill, P. M. W.; Johnson, B.; Chen, W.; Wong, M. W.; Andres, J. L.; Gonzalez, C.; Head-Gordon, M.; Replogle, E. S.; Pople, J. A. *Gaussian98*; Gaussian, Inc.: Pittsburgh, PA, 1998.
(55) Bayly, C. I.; Cieplak, P.; Cornell, W. D.; Kollman P. A. A well-behaved electrostatic potential based method using charge restraints for determining atom-centered charges: The RESP model. *J. Phys. Chem.* **1993**, *97*, 10269−10280.
(56) Callahan, T. J.; Swanson, E.; Lybrand, T. P. MD Display: An interactive graphics program for visualization of molecular dynamics trajectories. *J. Mol. Graph.* **1996**, *14*, 39−41.
(57) Meng, E. C.; Soichet, B. M.; Kuntz, I. D. Automated docking with grid-based energy evaluation. *J. Comput. Chem.* **1992**, *13*, 505−524.
(58) Livingstone, C. D.; Barton, G. J. Protein sequence alignments: A strategy for the hierarchical analysis of residue conservation. *CABIOS* **1993**, *9*, 745−756.
(59) Sanner, M. F.; Olson, A. J.; Spehner, J.-C. Reduced surface: an efficient way to compute molecular surfaces. *Biopolymers* **1996**, *38*, 305−320.
(60) DINO: Visualizing Structural Biology, 2001 (http://www.dino3d.org).

JM0301437